VILNIUS UNIVERSITY
CENTER FOR PHYSICAL SCIENCES AND TECHNOLOGY

IRINA ČERNIUKĖ

FABRICATION AND INVESTIGATION OF THE HETEROSTRUCTURES BASED ON MANGANITES AND ORGANIC SEMICONDUCTORS

Summary of Doctoral Dissertation
Technological Sciences, Materials Engineering (08T)

Vilnius, 2016

Doctoral dissertation was prepared at Center for Physical Sciences and Technology in 2007 – 2015.

Scientific Supervisor

Assoc. prof. dr. Bonifacas Vengalis (Center for Physical Sciences and Technology, Technological Sciences, Materials Engineering – 08T).

The United Vilnius University and Center for Physical Sciences and Technology Doctoral Dissertation Committee in Materials Engineering:

Chairman

Prof. habil. dr. Antanas Feliksas Orliukas (Vilnius University, Technological Sciences, Materials Engineering – 08T).

Members:

Prof. dr. Algirdas Sužiedėlis (Center for Physical Sciences and Technology, Physical Sciences, Physics – 02P),

Dr. Donats Erts (University of Latvia, Technological Sciences, Materials Engineering – 08T),

Assoc. prof. dr. Voitech Stankevič (Center for Physical Sciences and Technology, Technological Sciences, Materials Engineering – 08T),

Dr. Šarūnas Meškinis (Kaunas University of Technology, Technological Sciences, Materials Engineering – 08T).

The official defense of the dissertation will be held at a public meeting of joint scientific council of Vilnius University and Center for Physical Sciences and Technology on 29 February 2016 at 11.00 in the conference hall 206 of Semiconductor Physics Institute.
Address: Goštauto 11, Vilnius, Lithuania.

The summary of the doctoral dissertation was distributed on 29 January 2016.

A copy of the doctoral dissertation is available for review at the Library of Center for Physical Sciences and Technology Semiconductor Physics Institute and Vilnius University and VU web page address: *www.vu.lt/lt/naujienos/ivykiu-kalendorius*

VILNIAUS UNIVERSITETAS
FIZINIŲ IR TECHNOLOGIJOS MOKSLŲ CENTRAS

IRINA ČERNIUKĖ

MANGANITŲ IR ORGANINIŲ PUSLAIDININKIŲ PLONASLUOKSNIŲ DARINIŲ GAMINIMAS IR TYRIMAS

Daktaro disertacijos santrauka
Technologijos mokslai, medžiagų inžinerija (08T)

Vilnius, 2016

Disertacija rengta 2007–2015 metais Fizinių ir technologijos mokslų centre.

Mokslinis vadovas - doc. dr. Bonifacas Vengalis (Fizinių ir technologijos mokslų centras, technologijos mokslai, medžiagų inžinerija – 08T).

Disertacija ginama jungtinėje Vilniaus universiteto ir Fizinių ir technologijos mokslų centro Medžiagų inžinerijos mokslo krypties taryboje:

Pirmininkas – prof. habil. dr. Antanas Feliksas Orliukas (Vilniaus universitetas, technologijos mokslai, medžiagų inžinerija – 08T).
Nariai:

Prof. dr. Algirdas Sužiedėlis (Fizinių ir technologijos mokslų centras, fiziniai mokslai, fizika – 02P);

Dr. Donats Erts (Latvijos universitetas, technologijos mokslai, medžiagų inžinerija – 08T);

Doc. dr. Voitech Stankevič (Fizinių ir technologijos mokslų centras, technologijos mokslai, medžiagų inžinerija – 08T);

Dr. Šarūnas Meškinis (Kauno technologijos universitetas, technologijos mokslai, medžiagų inžinerija – 08T).

Disertacija bus ginama viešame Medžiagų inžinerijos mokslo krypties tarybos posėdyje 2016 m. vasario mėn. 29 d. 11 val. Fizinių ir technologijos mokslų centro Puslaidininkių fizikos instituto posėdžių salėje, k 206.
Adresas: Goštauto g. 11, Vilnius, Lietuva.

Disertacijos santrauka išsiuntinėta 2016 m. sausio mėn. 29 d.

Disertaciją galima peržiūrėti Fizinių ir technologijos mokslų centro Puslaidininkių fizikos instituto ir Vilniaus universiteto bibliotekose bei VU interneto svetainėje adresu: *www.vu.lt/lt/naujienos/ivykiu-kalendorius*

Introduction

Great attention is currently focussed on the development of new fields of electronics such as spin-dependent electronics (spintronics) and molecular electronics. Spintronics is a new rapidly developing research area exploiting spin-dependent electronic transport in various device structures based on magnetic materials while incorporation of hybrid organic – inorganic structures and even single molecules into electronics circuits is the main goal of molecular electronics.

Of key importance for the development of spintronics is the group of ferromagnetic (FM) materials exhibiting spin-polarized carriers and known as half metallic ferromagnets. The group includes colossal magnetoresistance manganites such as $La_{0,67}Ca_{0,33}MnO_3$ (LCMO), $La_{0,67}Sr_{0,33}MnO_3$ (LSMO), magnetite (Fe_3O_4), and other FM oxides [1,2]. Attempts are undertaken to prepare various multilayered device structures composed of ferromagnetic oxides, metallic, semiconducting and dielectric thin films. High magnetoresistance values and fast magnetic response make the heterostructures promising for fabrication of magnetic field sensors, magnetic random access memory elements (MRAM), magnetic field-driven optical devices and other devices.

Semiconductor *p-n* junction and Schottky diode (metal-semiconductor junction) are of key importance for Si-based electronics. One can expect that the combination of ferromagnetic oxides and organic semiconductors (OSC) could provide new electrical and magnetic functionalities into a single integrated device. Therefore elaboration of device structures containing FM oxides and OSC materials such as magnetic *p-n*, *p-i-n* diode structures as well as FM/I/FM tunnelling heterostructures containing barrier (I) from dielectric or OSC materials could be a basic issue for novel devices. The main advantage of organic materials is relatively simple and low temperature processing of their thin films through inexpensive techniques such as thermal evaporation, drop-casting and spin coating. Furthermore, OSC materials are composed of light elements and demonstrate unusually large values of spin relaxation time. It means that spin-polarized carriers could be directly injected into OSC from ferromagnetic electrodes or generated via photoexcitation by a circularly polarized light. This provides an interesting possibility for the development of new magnetic field-driven optoelectronic devices [3].

Though several hybrid device structures containing OSC and ferromagnetic materials have been reported and some applications of their properties have been pointed out, more attention needs to be focused on both preparation and complex investigation of heterostructures based on magnetic oxides as manganites and organic compounds. More attention could be paid also to integration of the ferromagnetic oxides into Si-based electronic circuits. There is also a great need to elucidate possible mechanisms of electrical transport at the interfaces of the heterostructures.

In this work, thin films and heterostructures based on $La_{0,67}Sr_{0,33}MnO_3$ (LSMO) and $La_{0,67}Ca_{0,33}MnO_3$ (LCMO) manganites and several OSC compounds were grown by various methods on crystalline MgO, *n*-$SrTiO_3$<Nb> (STON), *n*-Si and *p*-Si substrates. Structural quality of the prepared films has been investigated. Major attention was paid to electrical and magnetoresistive properties of both manganite films and the prepared *p-n* and *p-i-n* diode structures.

Major goals of this work

- To investigate variation of crystalline quality, electrical and magnetotransport properties of (001)-plane textured and polycrystalline LSMO thin films grown by magnetron sputtering at various temperatures (T_s=550÷800°C) on single crystal MgO(001) substrates.
- To reveal a role of grain boundaries on magnetotransport properties of polycrystalline LSMO/MgO films at low ($\mu_0 H$<0.2T) and high ($\mu_0 H$>0.2T) magnetic fields.
- To elucidate electrical and magnetoresistive properties of the Ag/LSMO point-like contacts.
- To elaborate technology for the preparation of heterostructures based on manganites (LSMO, LCMO) and organic semiconductors, namely, Alq_3, organic compounds based on naphthalene diimide and perimidine and to investigate electrical properties of the prepared hybrid diode structures.

Novelty of scientific investigation

- A role of grain boundaries (GB) on both electrical resistance and magnetoresistance of polycrystalline LSMO films grown at various temperatures on lattice mismatched crystalline MgO(001) substrates has been elucidated.
- Thin films of several organic semiconductors compounds based on naphthalene diimide and perimidine as well as related diode M/OSC/*n*,*p*-Si heterostructures have been grown by applying spin coating and vacuum evaporation technologies. Electrical properties of the prepared hybrid diode structures have been investigated.

Importance for application

- Technology of hybrid device structures containing thin films of manganites and organic semiconductors has been developed. The performed investigations demonstrate new possibilities to use the hybrid device structures for needs of electronics and spintronics.
- The prepared LCMO/YSZ/*n*-Si heterostructures demonstrating nonlinear and asymmetric current versus voltage relationships typical for high quality Schottky diode show promising possibilities for integration of the manganite films into Si-based integrated circuits.
- Magnetoresistive properties of point-like Ag/LSMO contacts demonstrate new possibilities for the elaboration of small-scale magnetic field sensors operating at room temperature.

Statements carried out for defense

1. Electrical properties of polycrystalline LSMO/MgO films at low temperatures ($T<<T_C$), are defined mainly by grain boundaries. Magnetoresistive properties of the films caused by grain boundaries either at low ($\mu_0 H<0.2$T) or high ($\mu_0 H>0.2$T) magnetic fields can be understood assuming current flow via two parallel channels caused by phase separation effect in the intergrain media.
2. Electrical and magnetoresistive properties of point-like Ag/LSMO contact are caused mainly by the so-called spreading resistance originating from a small volume of the manganite material at the Ag/LSMO interface caring the highest current density.
3. Enhanced Schottky barrier values of hybrid Al/Alq_3/*n*-Si, Al/Alq_3/*p*-Si diode structures (0.9 eV ÷ 1.1 eV and 0.77 eV ÷ 0.91 eV, respectively) compared to the corresponding values estimated for the Al/*n*-Si and Al/*p*-Si) diode structures (0.68 eV and 0.77 eV, respectively) demonstrate importance of charged dipole caused by polar Alq_3 molecules on the barrier formation.
4. High quality Schottky junctions with reduced leakage current may be fabricated by magnetron sputtering of the LCMO or LSMO films on lattice-matched crystalline *n*-$SrTiO_3$<Nb> substrates. Shunting resistance of similar LCMO/*n*-Si and LSMO/*n*-Si diode structures may be reduced significantly by introducing thin ($d \leq 5$ nm) interlayers of the dielectric $LaMnO_3$ (LMO) and Y_2O_3(8 mol % ZrO_2) (YSZ) oxides.

Publication and approbation of the scientific results

Major results of the thesis are represented in 4 referred scientific papers and 4 papers published as proceedings of international conferences. Major results of the work were also announced in a number of national and international conferences:

Publications in Journals exhibiting ISI index

1. K. Šliužienė, **I. Černiukė**, R. Butkutė, V. Lisauskas, B. Vengalis, S. Tamulevičius, M. Andrulevičius, R. Lygaitis, J. Gražulevičius, A. Undzėnas, Formation and electrical properties of metal/organic semiconductor/Si heterostructures based on naphthalene diimide-based compounds, *Molecular crystals and liquid crystals*, Vol. 497, pp. 154/[486]-163/[495] (2008). ISSN 1542-1406. doi:10.1080/15421400802459009.
2. **I. Černiukė**, K. Šliužienė, G. Grigaliūnaitė-Vonsevičienė, V. Lisauskas, A. Maneikis, B. Vengalis, Influence of preparation conditions on the electrical properties of the Al/Alq_3/Si diode structures, *Materials science (Medžiagotyra)*, Vol. 19, No. 4, pp. 363-366 (2013). ISSN 1392-1320. doi:10.5755/j01.ms.19.4.2733.
3. B. Vengalis, **I. Černiukė**, A. Maneikis, A.K. Oginskis, G. Grigaliūnaitė-Vonsevičienė, Electrical resistance and magnetoresistance of highly oriented and polycrystalline $La_{0,67}Sr_{0,33}MnO_3$/MgO_3/MgO(001) thin films, *Lithuanian Journal of Physics*, Vol. 55, No. 2, pp. 132-141 (2015). ISSN 1648-8504.

4. **I. Černiukė**, B. Vengalis, A. Steikūnienė, G. Grigaliūnaitė-Vonsevičienė, A.K. Oginskis, Electrical and magnetoresistive properties of the Ag/$La_{2/3}$,$Sr_{1/3}MnO_3$ point-probe contacts, *Lithuanian Journal of Physics*, Vol. 55, No. 1, pp. 17-23 (2015). ISSN 1648-8504.

Publications in conference proceedings

1. B. Vengalis, K. Šliužienė, **I. Černiukė**, R. Butkutė, V. Lisauskas, A. Maneikis, Preparation and properties of hybrid bilayer structures based on organic Alq_3, ferromagnetic $La_{2/3}Sr_{1/3}MnO_3$ and Fe_3O_4, Proc. of SPIE Vol. 7142, pp. 71420V(1-6) (2008). doi:10.1117/12.815942.
2. B. Vengalis, K. Šliužienė, V. Lisauskas, R. Butkutė, A. Maneikis, F. Anisimovas, A.K. Oginskis, V. Pyragas, **I. Černiukė**, J. Devenson, A. Steikūnienė, N. Šiktorovas, Įvairialyčiai magnetinių oksidų dariniai. Puslaidininkių fizikos instituto XIX mokslinės konferencijos darbai, sausio 8-10, 2008, Vilnius. Vilnius : PFI, pp. 93-96 (2008). ISBN 9789955750024.
3. **I. Černiukė**, K. Šliužienė, R. Butkutė, V. Lisauskas, A. Maneikis, A. Tomkevičienė, B. Vengalis, Organinio puslaidininkio ir silicio heterodarinių auginimas ir tyrimas. 11-osios Lietuvos jaunųjų mokslininkų konferencijos "Mokslas - Lietuvos ateitis" 2008 m. teminių konferencijų straipsnių rinkinys/Vilniaus Gedimino technikos universitetas. Vilnius: Technika, pp. 55-64 (2008). ISBN 978-9955-28-301-0.
4. K. Šliužienė, V. Lisauskas, **I. Černiukė**, G. Grigaliūnaitė-Vonsevičienė, B. Vengalis, R. Lygaitis, J.V. Gražulevičius, Preparation and electrical properties of the heterojunctions formed by growing organic semiconductor films on Si and $SrTiO_3$<Nb> substrates. 4th International conference: Radiation interaction with material and its use in technologies, May 14-17, 2012, Kaunas. Kaunas : Technologija, pp. 201-204 (2012). ISSN 1822-508X.

Participation in Conferences

1. K. Šliužienė, **I. Černiukė**, R. Butkutė, V. Lisauskas, B. Vengalis, S. Tamulevičius, R.Lygaitis, J.V.Gražulevičius, A.Undzėnas, Formation and electrical properties of metal/organic semiconductor/si heterostructures. 7th International conference: Electronic processes in organic materials, May 26-30, 2008, Lvovas, Ukraina. Kyiv, pp. 59-60 (2008). ISBN 9789666755400.
2. B. Vengalis, K. Šliužienė, **I. Černiukė**, R. Butkutė, V. Lisauskas and A. Maneikis, Preparation and Properties of Hybrid $La_{2/3}Sr_{1/3}MnO_3$/Organic Semiconductor structures. 6^{th} International conference (AOMD-6), August 24-27, 2008, Riga, Latvia. Programme and abstracts, Riga, p. 22 (2008).
3. **I. Černiukė**, K. Šliužienė, G. Grigaliūnaitė-Vonsevičienė, V. Lisauskas, A. Maneikis, B. Vengalis, Influence of preparation conditions on the electrical properties of the Al/Alq_3/Si diode structures. 14th International Conference-School: Advanced materials and technologies, August 27-31, 2012, Palanga. Kaunas : Technologija, p. 43 (2012). ISSN 1822-7759.
4. B. Vengalis, A. K. Oginskis, **I. Černiukė**, G. Grigaliūnaitė-Vonsevičienė and A. Maneikis, Electrical and magnetoresistive properties of the metal-$La_{0,67}Sr_{0,33}MnO_3$

interface. 15th International Symposium on Ultrafast Phenomena in Semiconductors: August 25-28, 2013, Vilnius. Vilnius : PFI, p. 64 (2013). ISBN 9786099551111.
5. **I. Černiukė**, A. K. Oginskis, K. Steikūnienė, V. Lisauskas, G. Grigaliūnaitė-Vonsevičienė, B. Vengalis, Nonlinear electrical properties and magnetoresistance of M-$L_{2/3}$(Ca, Sr)$_{1/3}$MnO (M= Ag, Ni) heterojunction. 15th International Conference-School: Advanced materials and technologies, August 27-31, 2013, Palanga. Kaunas : Technologija, p. 95 (2013). ISSN 1822-7759.
6. **I. Černiukė**, B. Vengalis, G. Grigaliūnaitė-Vonsevičienė, Low field magnetoresistance anomaly in $La_{0.67}Sr_{0.33}MnO_3$ thin films. 16th International Conference-School: Advanced materials and technologies, August 27-31, 2014, Palanga. Kaunas : Technologija, p. 82 (2014). ISSN 1822-7759.
7. **I. Černiukė**, B. Vengalis, G. Grigaliūnaitė-Vonsevičienė, K. Šliužienė, A. Maneikis, Plonųjų $La_{2/3}Sr_{1/3}MnO_3$ sluoksnių magnetovaržinės savybės silpnuose magnetiniuose laukuose. 41-oji Lietuvos nacionalinė fizikos konferencija, birželio 17-19 d. 2015, Vilnius. Vilnius : FTMC, p. 315 (2015). ISBN 9786099551128.

Content of the thesis

The thesis consists of six chapters including Introduction (Chapter 1), Methodology (Chapter 2) and four original chapters (3-6). Short introduction and major goals of the performed investigations as well as conclusions are presented in each original chapter while the most important conclusions of the work and list of references are summarised in the end of the thesis.

Structure of the thesis, short introduction of the problems to be solved, main goals of the investigations, scientific novelty, practical importance and statements carried out for defense are presented in the **Introduction.**

The first chapter presents a review of main properties of the manganites including their crystalline structure, phase diagrams and electrical transport. Major attention is paid to electrical and magnetic properties of the lanthanum manganites used in this work for the preparation of heterostructures. This chapter also presents list of the most important publications.

In the second chapter one can find general description of the methods used for the preparation, characterization and investigation of thin films and related heterostructures based on manganites and organic semiconductors.

In the third chapter attention is paid to the formation and investigation of the LSMO thin films. The goal was to investigate possible variation of magnetotransport properties of (001)-plane textured LSMO thin films when grown by magnetron sputtering on single crystal MgO(001) substrates exhibiting significant lattice mismatch (of about 8.0 %) in respect to the film material. The LSMO films exhibiting highly (001)-plane oriented and polycrystalline structure with a variable amount of (011)-textured crystallites have been grown *in-situ* by magnetron sputtering on crystalline MgO(001) substrates by changing deposition temperature from 550°C to 800°C. Competing contribution of grains and grain boundaries on resistivity and magnetoresistance of the films has been investigated at T = (78÷330) K.

Typical AFM surface images of two LSMO films grown on MgO substrates at 800ºC and 600ºC are displayed in Fig.1a,b. The averaged surface roughness of the films ranged from 2.51 nm for the L800 film to about 4.22 nm for the L550 film.

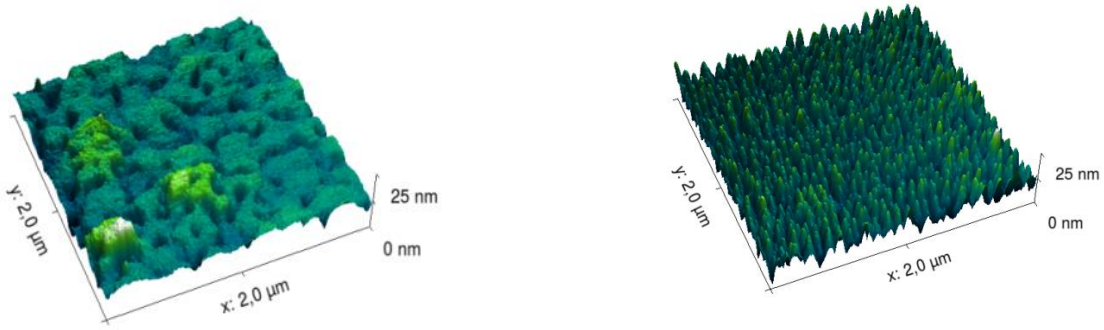

a) b)

Fig.1a,b. AFM surface images of the L800 and L600 films grown on MgO(001) substrates at 800 ºC (a) and 600ºC (b).

The averaged grain size estimated for various films was found to decrease from about 286 nm to 45 nm with substrate temperature, T_s, decreasing from 800°C to 550°C (Table 1).

Table 1. Thickness, d_f, average roughness, R, and grain size, d_G, of the LSMO films grown at different substrate temperatures, T_s, as found from AFM surface images.

T_s, °C	800	750	700	650	600	550
d_f, nm	210	180	220	215	195	160
R, nm	2.51	2.83	2.60	3.2	3.95	4.22
d_G, nm	286	133	95	69	57	45

Resistivity versus temperature, $\rho(T)$, of the LSMO films grown on MgO(001) substrates at different temperatures (T_s = 550÷800°C) is shown in Fig.2a. Gradual

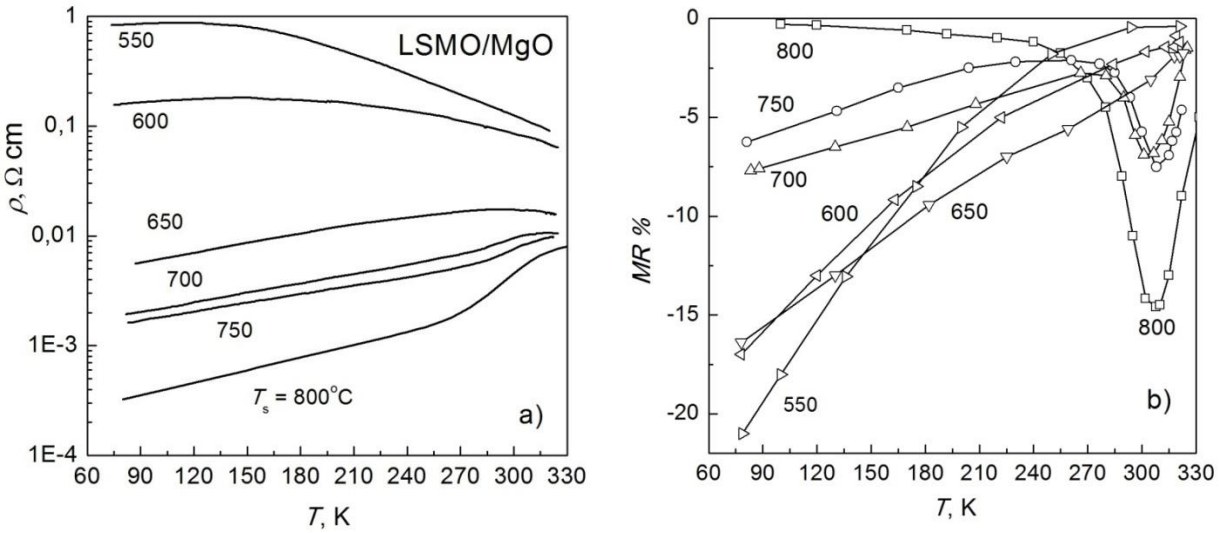

Fig.2a,b. Resistivity (a) and magnetoresistance ($\mu_0 H_{\parallel}$ = 0.73 T) (b) vs temperature measured for the LSMO films grown on MgO substrates at different temperatures, T_s = 550÷800 ºC. Lines in (b) are easy traces for an eye.

increase of ρ with T_s decreasing from 800°C to 550°C demonstrate increasing role of grain boundaries on resistivity of the grown polycrystalline films.

Magnetoresistance, $MR = [R(H) - R(0)]/R(0)]$, measured for the same films at a fixed magnetic field ($\mu_0 H_{||} = 0.73$ T) applied parallel to a film plane is shown in Fig.2b. We point out peak-like $MR(H)$ anomalies with the highest negative MR of about 14% measured at $T = 305$ K for the highest crystalline quality L800 film. Polycrystalline films grown at 750°C, 700°C and 650°C showed similar $MR(T)$ anomalies with reduced peak amplitudes while negligible small MR values have been measured in the same temperature range for the films grown at low temperatures ($T_s = 600$°C and 550°C).

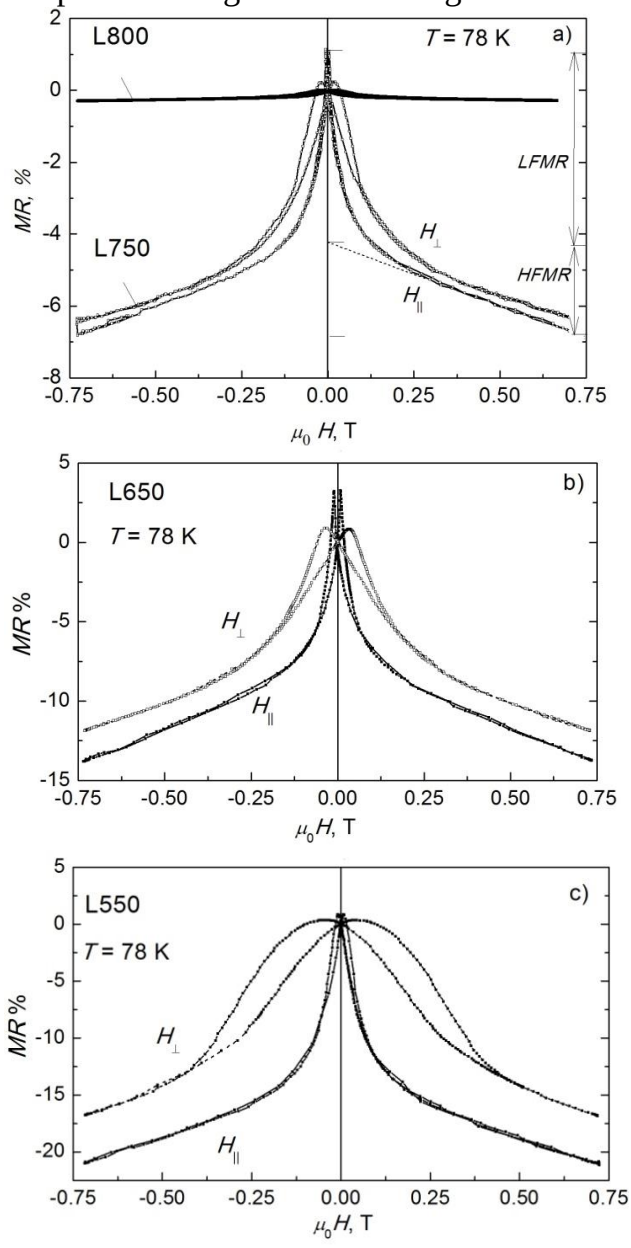

Fig.3a,b,c. Magnetic field-dependent magnetoresistance measured at 78K for highly oriented L800 film (a) and polycrystalline L750 (a), L650 (b), L550 (c) films. Magnetic field was applied parallel ($H_{||}$) and normal ($H_{\perp}$) to a film plane.

MR of highly oriented L800 film and polycrystalline L750, L650, L550 films measured at 78 K as a function of magnetic field applied parallel ($H_{||}$) and normal ($H_{\perp}$) to a film plane is displayed in Fig.3a,b,c. Following the figure we point out: 1) clearly defined peak-like $MR(H)$ anomalies at low magnetic fields ($\mu_0 H < 0.25$ T), 2) significant hysteresis of the $MR(H)$ curves, 3) MR anisotropy with applying magnetic field parallel and normal to a film plane, and 4) almost linear $MR(H)$ behaviour for all the films at high magnetic fields ($\mu_0 H > 0.25$ T). Enhanced resistivity of all LSMO films grown in this work at lower temperatures we associate with high angle grain boundaries which may be formed between dominating (001)-oriented grains and certain relatively small amount of grains with (011) or other textures. Enhanced electrical resistivity of polycrystalline manganite film, $\rho(T)$, with current flowing via an array of grains and grain boundaries can be understood by applying a simple quasi-linear (1D) approximation:

$$\rho(T) = \rho_G(T) + \left(\frac{d_{GB}}{d_G}\right)\rho_{GB}(T), \qquad (1)$$

here $\rho_G(T)$ and $\rho_{GB}(T)$ represent partial resistivity defined by grains and highly resistive GBs, d_G, d_{GB} are the averaged dimensions of grains and grain boundaries, respectively. It has been assumed for simplicity that $d_{G,} >> d_{GB.}$

To reveal additional resistivity of polycrystalline LSMO films governed by GBs, in Fig.4 are shown the $\Delta\rho(T)$ plots obtained for various films by eliminating contribution of internal grain resistivity of the highest crystalline quality L800 film from the corresponding $\rho(T)$ curves displayed in Fig.2a. Correlation of $\Delta\rho$ with the inverse grain size, $1/d_G$, (see Table 1) at T=300 K and 78 K is shown in Fig.5.

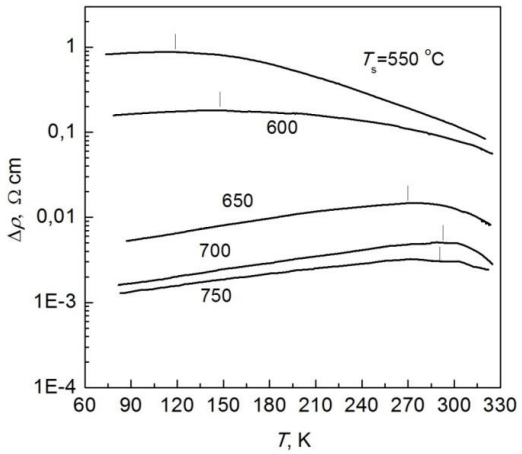

Fig.4. Temperature-dependent additional resistivity of polycrystalline LSMO films, $\Delta\rho$, evaluated by eliminating internal resistivity of the highest crystalline quality L800 film from the corresponding $\rho(T)$ plots in Fig. 5a.

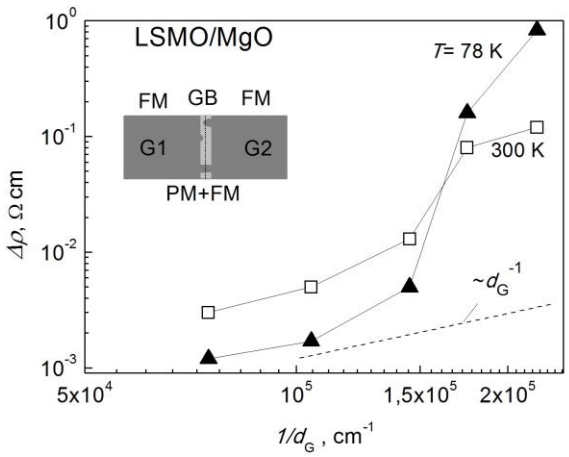

Fig.5. The grain boundary-governed additional resistivity of various polycrystalline LSMO films at T = 78 K and 300 K as a function of the inverse grain size, $1/d_G$. Simplified drawing of GB model suggesting phase separated state at GBs and possible carrier transport across GBs via two parallel channels is shown in the inset.

The following expression has been obtained from (1) to estimate *MR* of a polycrystalline manganite film:

$$MR = \alpha MR_G + (1-\alpha)MR_{GB}, \qquad (2)$$

here MR_G and MR_{GB} are constituent parts of film magnetoresistance defined by grains and grain boundaries, respectively, and $\alpha = \rho_G/\rho$.

We point out a key importance of the well known phase separation phenomenon in the intergrain region to explain spatially nonuniform current flow via GBs. Favorable conditions for phase-separated state at GBs exist due to a number of factors as reduced carrier density, nonuniform strains caused by a substrate and possible microscopic structural nonhomogeneities [4]. Taking into account reduced carrier density in the intergrain region, it was assumed that FM state in the vicinity of GBs at $T < T_C$ appears in a form of FM clusters with a fixed carrier density embed in highly resistive PM matrix. Schematic drawing of a single GB (at $T < T_c$) demonstrating coexistence of highly conductive (FM) and highly resistive (PM) regions at the interface between the adjacent misoriented FM grains G1 and G2 is shown in the inset to Fig.5.

The forth chapter presents electrical and magnetoresistive properties of Ag point-probe contacts formed by attaching bent Ag wire to a top of highly oriented LSMO thin film grown by magnetron sputtering at 800° C.

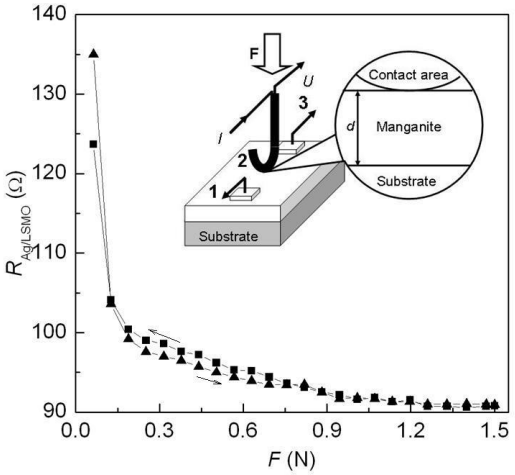

Fig.6. Contact resistance of the Ag probe electrode measured at 295 K by 3 point-probe method with load force, *F*, increasing and decreasing gradually in the range 0 ÷ 1.5 N. Schematic drawing of 3 point-probe measurement circuit is displayed in the inset.

Fig.6 shows typical variation of contact resistance ($R_{Ag/LSMO}$) measured at 295 K by applying 3-probe method with load force, *F*, increasing and decreasing gradually in the range 0 ÷ 1.5 N.

Resistance of the LSMO film, R_{LSMO}, and that of contact resistance, $R_{Ag/LSMO}$, both measured in the absence of magnetic field (solid lines) and at a magnetic field ($\mu_0 H_{//}$ = 0.73 T) directed parallel to a film surface (dotted lines) are shown in Fig.7a. The R_{LSMO} and $R_{Ag/LSMO}$ versus temperature plots displayed in Fig.7a are normalized to the maximal zero field values.

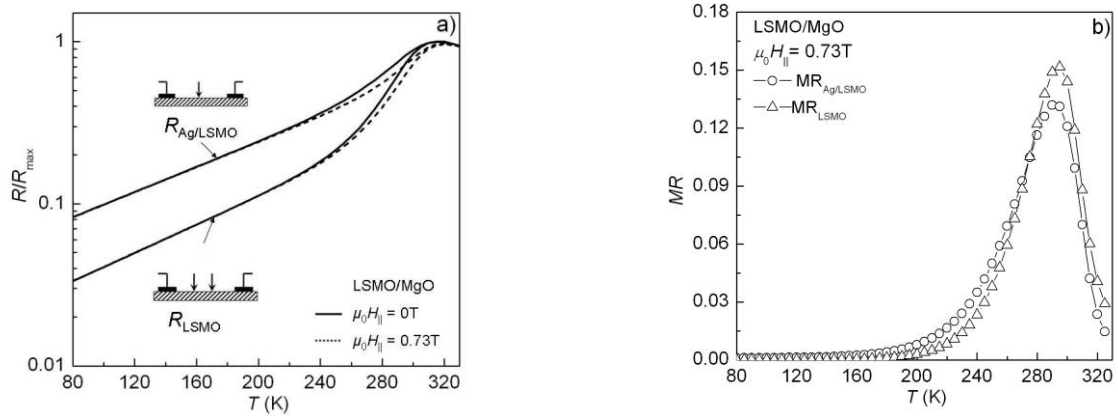

Fig.7a,b. Resistance of the LSMO film and that of the Ag/LSMO contact normalized to maximal zero field values (a), and contact magnetoresistance ($MR_{Ag/LSMO}$) (b) measured under magnetic field $\mu_0 H_{||}$ = 0.73T directed parallel to the film plane.

Slightly lower maximal value of contact magnetoresistance, $MR_{Ag/LSMO}$, of about 13% compared to maximal film magnetoresistance (~15%) may be a result of a possible ultrathin surface layer with lowered carrier density and reduced magnetic properties that is a common feature of most manganite films.

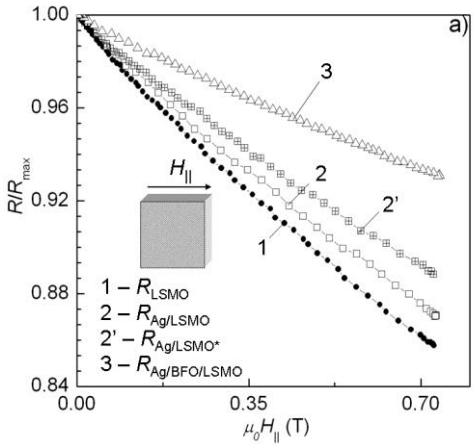

Fig.8. In-plane LSMO film resistance (1) and contact resistance of the Ag/LSMO (2), Ag/LSMO* (2') and Ag/BFO/LSMO (3) junctions measured at T = 295 K and normalized to the corresponding zero field values. Magnetic field directed parallel ($H_{||}$) to the film plane (b).

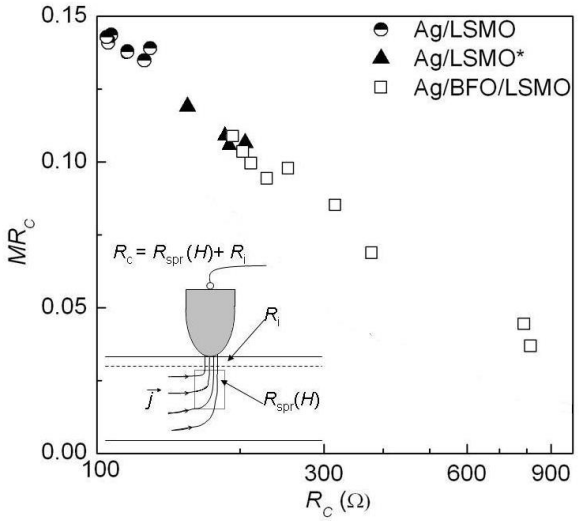

Fig.9 Magnetoresistance of various contacts (MR_c) at the applied magnetic field $\mu_0 H_{||}$ = 0.73T versus contact resistance (R_c) measured at T = 295 K for the Ag/LSMO and Ag/BFO/LSMO junctions.

Junction resistance of various point-like Ag contacts measured at T = 295 K as a function of magnetic field directed parallel ($H_{||}$) to the film plane is shown in Fig.8.

Fig.9 shows a clear correlation between sets of contact resistance and contact magnetoresistance values ($\mu_0 H_{||}$ = 0.73T) measured at T = 295 K for three kinds (Ag/LSMO, Ag/LSMO* and Ag/BFO/LSMO) contacts. Note that LSMO* is the film that was kept in air during 1 month after deposition

It was found that keeping the samples in air ambient for 1 month resulted slight increase of R_c and decrease of MR_c values due, probably, to additional loss of oxygen from LSMO surface and development of highly resistive surface layer. At the same time, presence of highly resistive ultrathin BFO overlayer resulted significant increase of contact resistance and decrease of contact magnetoresistance values. We argue that in a general case contact resistance for small area contacts might be considered consisting of two parts according to equation (3):

$$R_{Ag/LSMO}(H) = R_{spr}(H) + R_i , \qquad (3)$$

here $R_{spr}(H)$ is magnetic field-dependent spreading resistance that is a common feature of small interface area electrodes [5] and R_i is temperature-dependent additional resistance that can be related either to a possible highly resistive surface layer (with reduced oxygen content, lowered carrier density and reduced magnetic order parameter) or additionally evaporated overlying film of nonmagnetic material. Taking into account relatively large contact resistance values ($R_c \sim 100\ \Omega$) in a case of small interface, importance of spreading resistance (R_{spr}) [5] for both resistance and magnetoresistance of the Ag/LSMO contacts has been pointed out.

In the fifth chapter we report synthesis of two organic polymers: POANT containing electronically isolated 1,4,5,8-naphthalenetetracarboxylic diimide units and FCAND – a low-molar-mass compound with two different (fluorenone and 1,4,5,8-naphthalenetetracarboxylic diimide) electron accepting units and three naphthalene diimide–based organic polymers: POANT, FCAND and PEPK (oligomeric *p*-type

semiconductor). Attention was also undertaken on a comparative study of metal/organic semiconductor/Si heterostructures based on thin films of the OSC mentioned above. Highly doped *n*- and *p*-type silicon substrates were used as an inorganic counterpart of the heterojunctions. The Alq_3, FCAND and PEPK films (d = 100 ÷ 300 nm) were thermally evaporated in vacuum ($p \approx 4\times10^{-6}$ Torr) onto non-heated Si substrates. The POANT and FCAND layers (d = 200 ÷ 500 nm) were prepared by spin coating technique using 5% and 2% chloroform solutions, respectively, followed by drying for 3–4 h at 150°C.

AFM surface images of the prepared organic PEPK, POANT and FCAND films are displayed in Fig.10a,b,c, respectively.

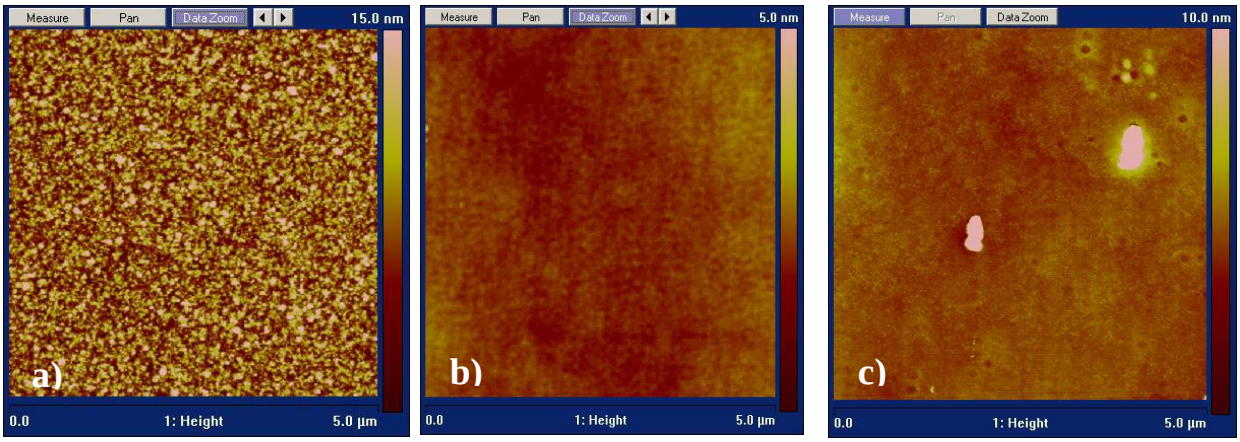

Fig.10a,b,c Surface morphology AFM images of organic films on Si substrates: (a) PEPK film (d = 0.3 µm) prepared by thermal evaporated in vacuum, POANT (d = 0.3 µm) (b) and FCAND (d = 0.3 µm) (c) films prepared on Si by spin coating.

The prepared hybrid organic on inorganic semiconductor heterojunctions demonstrated nonlinear *I-U* dependencies and clearly defined rectifying properties (see Fig.11) indicating that the heterojunctions behave like a Schottky (metal/semiconductor) contact.

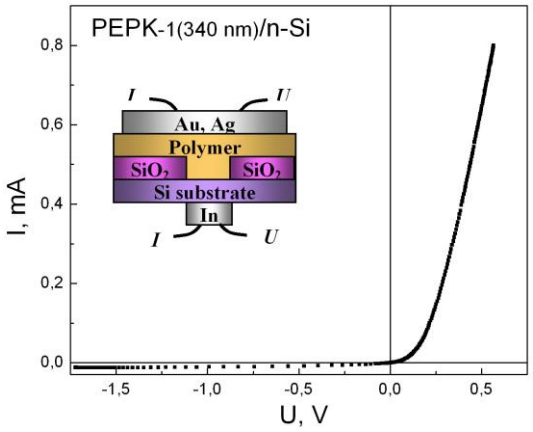

Fig.11. Typical current versus voltage dependence measured for the PEPK/*n*-Si heterojunction at 290 K. Schematic view of the sample is shown in the inset.

Fig.12 shows semi-log plot of current-voltage (*I–U*) characteristics measured for the Ag/EBC/*n*-Si device structures at room temperature in a case of a forward (1) and reverse (2) bias.

Linear *I-U* relations measured for the heterojunctions at low bias voltages ($|U| \leq$ 0,1 V) demonstrate certain shunting effect due, probably, to nonuniform thickness of the OS layer or possible diffusion of Ag into organic layers. However, nonlinear *I-U* behavior and clearly defined rectifying properties indicated at higher voltage values ($|U| \geq 0.1$ V) certify presence of interfacial potential barrier in the heterostructures. The observed exponential growth of current with a forward bias indicated in this work for the (BPBC, EBC)/(*n*-Si, STON) heterostructures showed unambiguously that all the device structures behave like a Schottky diode (metal-

semiconductor junction) with a potential barrier occurring in the interface between metallic Ag and inorganic (Si, STON) semiconductors with intermediate organic (BPBC, EBC) layers.

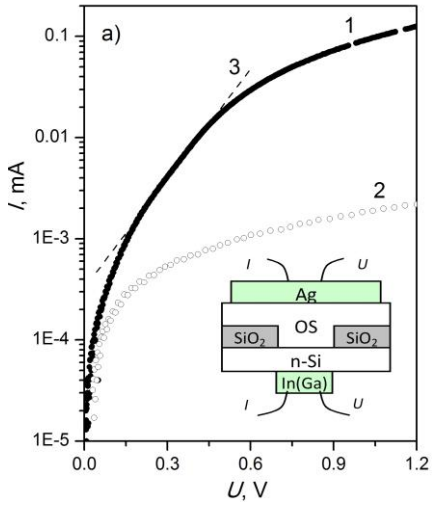

Fig.12. Typical current-voltage semi-log plots of the Ag/EBC/*n*-Si device structure measured at 293 K in a case of forward (1) and reverse (2) bias. (3) shows exponential *I-U* behaviour.

Typical forward *I-U* characteristics measured for the prepared Al/Alq_3/*p*-Si and Al/Alq_3/*n*-Si diode structures containing interlaying Alq_3 films of different thickness are displayed in Fig.13a,b, respectively

Exponential growth of current with forward voltage has been indicated both for the Al/Alq_3/*n*-Si and Al/Alq_3/*p*-Si heterostructures (see clearly defined linear portions over several orders of forward bias values in the semi-log *I-U* plots). Thus, one can conclude that all the heterostructures behave like a conventional Schottky diode (M-S junction).

Comparing results for the diode structures displayed in Fig.13a,b one can certify that insertion of ultrathin Alq_3 film results noticeable modification of electrical properties. Certainly, we point out reduced forward and reverse current values, increased zero bias resistance and improved rectification property of the hybrid organic-inorganic diode structures in comparison to Al/*n*-Si and Al/*p*-Si diodes without the intermediate OSC film.

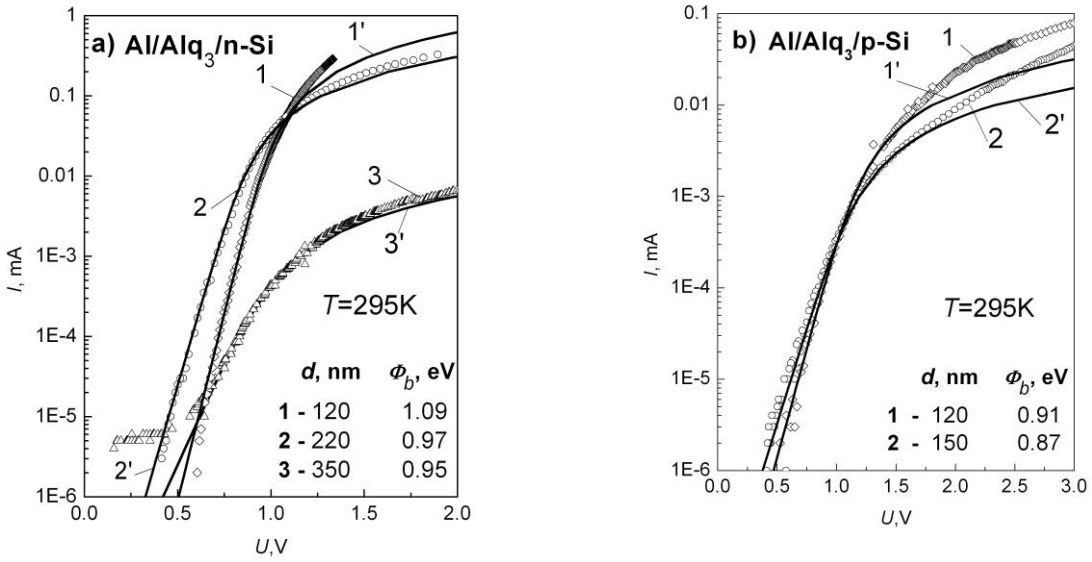

Fig.13a,b. Forward *I-U* characteristics measured at 295 K for the Al/Alq_3/*n*-Si (a) and Al/Alq_3/*p*-Si (b) heterostructures with thermally evaporated (1, 2) and spin coated (3) interlaying Alq_3 film. The corresponding fitting curves (1'-3') have been calculated using Schottky thermionic emission model.

Carrier transport in the prepared organic-inorganic diode structures has been modeled taking into account dominating role of Shottky thermionic emission. Current flowing through a uniform metal-semiconductor interface with applied forward bias due to the thermionic emission, can be expressed as [6]:

$$I = I_0\left[\exp\left(\frac{q(U - IR_S)}{nkT}\right) - 1\right], \quad (4)$$

$$I_0 = AA^*T^2 \exp\left(-\frac{q\Phi_b}{kT}\right), \quad (5)$$

here I_0 is the saturation current, q is the electron charge, U is the forward bias voltage, R_S is series resistance, n is ideality factor (n = 1 for an ideal contact), k is the Boltzmann constant, T - the absolute temperature. A is the effective area of the device structure, A^*- is the effective Richardson constant (32 $cm^{-2}K^{-2}$ for p-type Si, 112 A $cm^{-2}K^{-2}$ for n-type Si, 156 A $cm^{-2}K^{-2}$ for STON). The activation energy Φ_b (zero-bias barrier height) has been obtained from the equation (5) while I_0 has been derived from the current axis intercept of the linear regions in the forward bias (ln I–U) plots. Major electrical parameters of the POANT/p-Si, FCAND/n-Si and PEPK/n-Si heterostructures derived from the I-U plots are displayed in Table 2 while similar parameters for diode structures based on Alq_3 organic compound are summarized in Table 3.

Table 2. Major electrical parameters of the POANT/p-Si, FCAND/p-Si and PEPK/n-Si heterostructures derived from the I-U plots.

Organic material	**FCAND**	**POANT**	**PEPK**
Substrate	n-Si	p-Si	n-Si
Thickness, nm	300	100	220
Roughness (R_{ms}), nm	2.7	0.28	0.24
Ideality factor, n	3	2.9	2.5
Activation energy, eV	0.70	0.66	0.68
Saturation current density J_0, A/cm^2	$2\cdot10^{-7}$	$1\cdot10^{-6}$	$4\cdot10^{-7}$

Table 3. Electrical parameters of the diode structures: thickness of the interlaying Alq_3 film, d_{Alq3}, zero bias barrier height, Φ_b, ideality factor, n, series resistance, R_s, and the rectification ratio K (U=±1 V) estimated from the measured I-U plots.

Structure	d_{Alq3}, **nm**	Φ_b, **eV**	n	R_s, **kΩ**	K
Al/Alq_3/n-Si	85	1.10	1.55	0.4	1800
	110	1.00	1.90	0.6	2600
	100	0.92	2.30	0.4	1200
	150	1.09	1.60	1.4	700
	170	0.975	1.7	1.0	860
	180	0.95	2.00	1.4	1100
	200	0.90	2.0	1.8	3200
	220	0.97	2.10	3.2	2100
Al/Alq_3/n-Si (spin coating)	350	0.93	3.3	150.0	340
Al/Alq_3/p-Si	120	0.91	3.50	50.0	400
	90	0.80	2.7	23.0	500
	80	0.77	2.8	12.0	270
	150	0.87	3.8	10.0	400
	100	0.77	3.2	40.0	380
	200	0.82	3.5	110.0	250
Al/n-Si	0	0.77	2.20	0.18	180
Al/p-Si	0	0.68	2.45	0.16	250

In the sixth chapter we present fabrication and comparative study of *p-n* heterojunctions based on thin films of manganites and organic Alq_3 compound. The LSMO and LCMO films ($d \approx 100 \div 200$ nm) were grown *in-situ* at 750°C by magnetron sputtering on STON and phosphorus-doped *n*-Si(100) substrates with native SiO_2 oxide chemically removed just before deposition. while the organic films were prepared as top layers onto the oxide layers by thermal evaporation. The interfacial YSZ and LMO buffer layers have been prepared on STON and Si substrates by magnetron sputtering technique. Their thickness ($d \approx 5$ nm) was controlled by deposition time.

XRD spectra revealed epitaxial growth of all manganite films when grown on lattice-matched STON(100) substrates while single-phase polycrystalline films have been prepared under the same condition either on Si(111) substrates with removed SiO_2 layer and Si coated by YSZ and LMO layers. The films grown heteroepitaxially on STON substrates showed relatively smooth surface with average grain size of about 200 nm and surface roughness of 5 nm while similar AFM studies for the films on Si revealed smaller grains (d~100 nm) and slightly higher surface roughness (~ 5 nm).

Sets of the junctions with a fixed area of about 1 mm^2 were patterned by applying a conventional photolithographic technique and wet etching. The junction resistance, R_J, magnetoresistance and current-voltage (*I-U*) characteristics were measured for the heterostructures at T=(300÷78) K.

Nonlinear current-voltage (*I-U*) characteristics and clearly defined rectifying properties were indicated in this work for all the heterostructures in the whole temperature range (80÷300) K. The heterostructures based on both LSMO and LCMO films showed relatively low zero field junction resistance values compared to those LCMO films (see Table 4).

Linear parts of the forward ln*I-U* plots seen for the LCMO/STON and LCMO/YSZ/STON heterojunctions in Fig.14 and Fig.15, respectively, show dominating role of Schottky thermionic emission. Clearly defined linear ln*I-U* relations have been certified for the LCMO/YSZ/*n*-Si heterostructure while the LCMO/*n*-Si heterojunction without intermediate YSZ layer demonstrated linear *I-U* relation due to enhanced tunneling and the resultant relatively low shunting resistance values.

Table 4. Characterisation of the heterostructures: Curie temperature of the manganite layer - T_c, zero bias interface resistance, R_{J0}(300K), series series resistance R_{ser}(300K), and barrier height, V_{B0} (T=300K) derived from the ln*I-U* plots.

Heterostructure	Struct. quality	T_c, K	R_{J0}, Ω	R_{ser}, kΩ	V_{B0}, eV
p-LSMO/STON(100)	epit.	310	10^4	-	-
p-LCMO/STON(100)	epit.	252	$3 \cdot 10^4$	-	-
p-LCMO/STON(100)	epit.	175	$3 \cdot 10^5$	1.21	0.81
p-LCMO/YSZ/STON	(001) text.	200	$4 \cdot 10^5$	0.47	0.78
p-LCMO/*n*-Si(111)	polycryst.	150	~10^5	0.52	0.95
p-LCMO/LMO/*n*-Si	polycryst.	140	~10^7	0.60	0.82
p-LCMO/YSZ/*n*-Si	polycryst.	120	>10^7	0.47	0.78

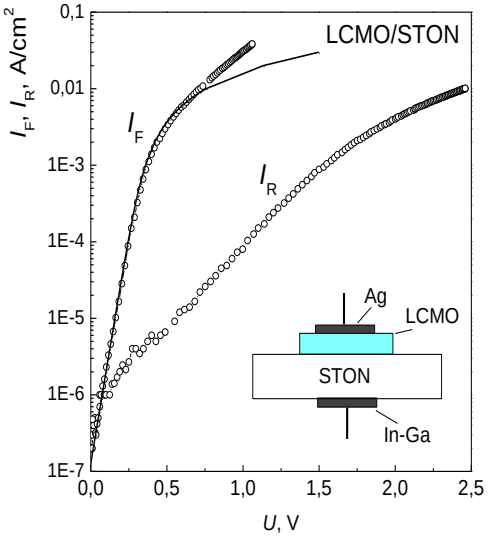

Fig.14. Forward (I_F) and reverse (I_R) currents versus applied voltage measured for the LCMO/STON heterojunction at 300 K.

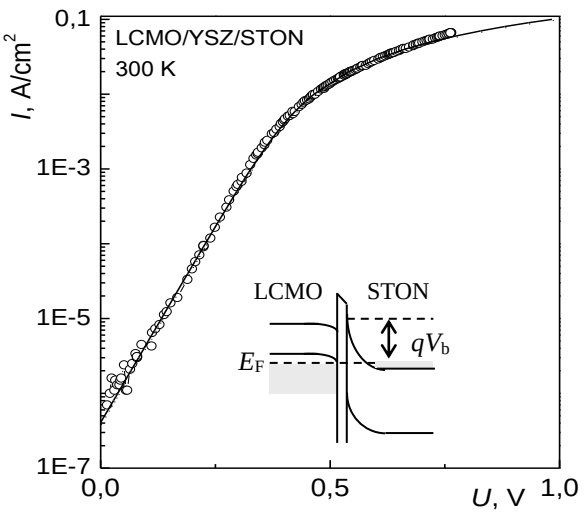

Fig.15. Semi-log *I-U* plot of the LCMO/YSZ/STON heterojunction measured at 300 K.

The measured *I-U* relations in a case of applied forward bias have been modeled taking into account Schottky thermionic emission and influence of both leakage current and series resistance as shown in the inset to Fig.16a.

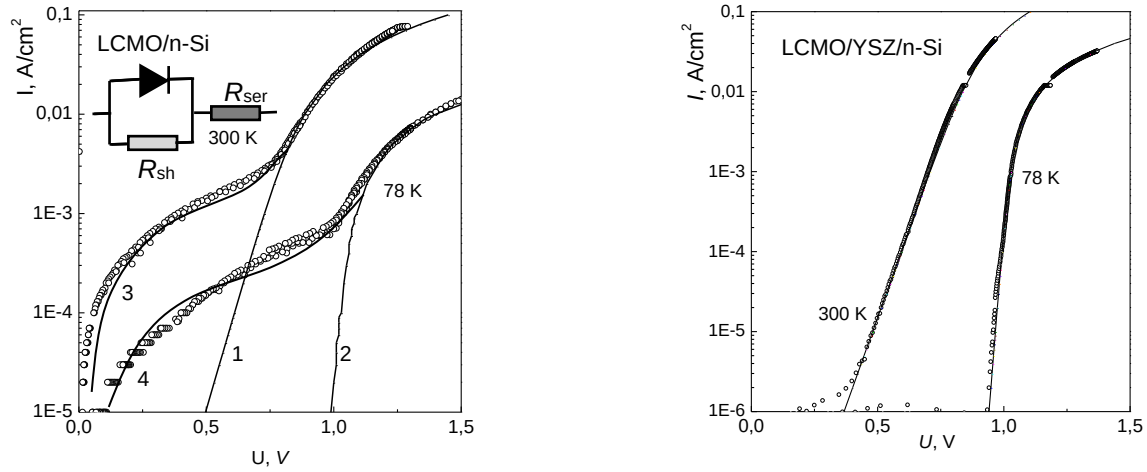

Fig.16a,b. Semi-log. *I-U* plots of the LCMO/*n*-Si (a) and LCMO/YSZ/*n*-Si (b) heterojunctions measured at 300 K and 78 K. Solid lines represent numerical curves calculated within the generalized Schottky junction theory (1,2) and taking into account shunting resistance, R_{sh} (3,4).

In Fig.17, we show the *I-U* dependences, measured for the Alq_3/LSMO heterojunctions at two different temperatures (T=295 K and 240 K) in the absence and presence of a magnetic field ($\mu_0 H$ =1.0 T). Temperature-dependent magnetoresistance of the Alq_3/LSMO interface (MR_J) measured by applying 3 point-probe method with current passing perpendicularly to a film plane (at $\mu_0 H$ =1.0 T) and magnetoresistance of the LSMO film (measured by applying current-in-plane geometry) are shown in Fig.18. It can be seen from this figure that the interface formed between LSMO and Alq_3 films demonstrated significant magnetoresistance values in a wide temperature range below Curie temperature of the LSMO film ($T_C \cong$ 290 K).

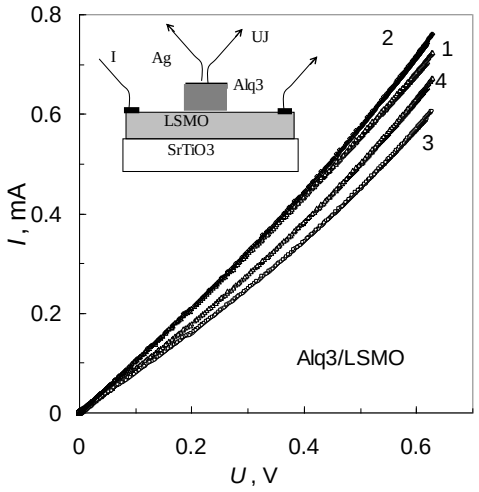

Fig.17. Current-voltage plots measured for the Alq_3/LSMO heterojunctions at T=295 K (1,2) and 240 K (3,4) in the absence (1, 3) and presence (2, 4) of magnetic field ($\mu_0 H$ =1.0 T).

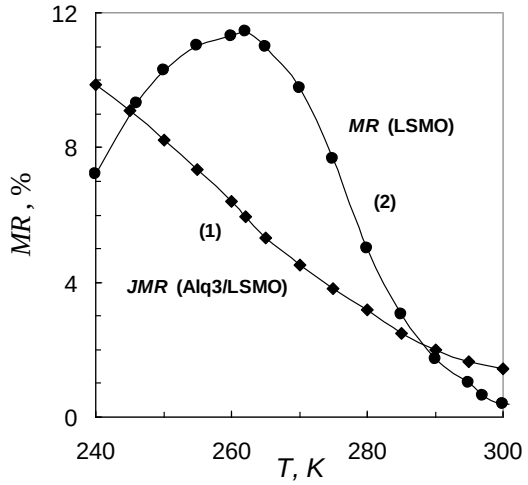

Fig.18. Magnetoresistance of the Alq_3/LSMO interface (1) and in-plane magnetoresistance of the LSMO film (2) ($\mu_0 H$ =1.0 T).

Nonlinear *I-U* relations and negligible rectifying behavior of the Alq_3/LSMO heterojunction (see Fig.17) has been explained assuming formation of a thin potential barrier (d ~ 1 nm) in the interface governing tunnelling of carriers between Alq_3 and the conductive manganites. Formation of such barrier in the heterostructures may be expected taking into account possible modification of chemical bonds at the interface and also reduction of oxygen content in the FM oxides during OSC film growth in vacuum. It was found, however, that numerical values of tunnelling current estimated by us from the well known Simons low [7] are significantly lower compared to those presented for the heterostructure in Fig.17.

It was assumed that charge transport in the hybrid diode structures is governed by space-charge-limited current process in the Alq_3 layer. Electrical transport through the organic thin film governed by a discrete trapping level in the band gap of an organic layer was estimated by applying the commonly used equation for space-charge limited current [8]:

$$J = \frac{9}{8}\varepsilon\mu\Theta\frac{U^2}{d^3}, \qquad (6)$$

here J and U are current density and applied voltage, μ, ε and d are the mobility of carriers, permittivity and thickness of the OSC layer, respectively, and Θ is the trapping parameter. One can conclude that a role of space charge is important when the density of injected charge carriers is much larger than the thermal-generated free-charge-carrier density. Certainly, carrier density in the FM oxides (~ 10^{21} cm^{-3}) is much lower compared to that in the Alq_3 compound.

MAIN RESULTS AND CONCLUSIONS

1. Highly (001)-plane textured LSMO thin films have been grown by magnetron sputtering on lattice mismatched MgO(001) single crystal substrates at 800°C while polycrystalline films containing additional (011)-plane oriented crystallites structure have been prepared on the same substrates at T=(550÷750)°C.
2. Competing contribution of grains and grain boundaries on temperature-dependent resistivity and magnetoresistance of the films have been elucidated. The highest negative *MR* values up to 14% at 300 K under magnetic field $\mu_0 H_{\parallel}$=0.73 T have been measured for highly oriented L800 films. Reduced *MR* values measured for all polycrystalline LSMO films (at 300 K) have been explained assuming additional magnetic field independent series resistance of grain boundaries.
3. The low field magnetoresistance effect in polycrystalline LSMO/MgO films has been explained assuming tunneling of spin-polarized carriers via tunnelling barriers formed naturally between misoriented grains. Significant high field magnetoresistance values measured for the films at $T<<T_C$ have been associated to magnetic field-dependent hopping of carriers via the intergrain regions with reduced carrier density.
4. A model based on two parallel channels of carrier transport across grain boundaries enables to explain coexistence of the low field magnetoresistance and high field magnetoresistance effects for polycrystalline LSMO films at low temperatures. The performed investigations revealed a key importance of phase separation phenomenon in the vicinity of GB on both microstructure and complex GB-governed magnetotransport phenomena in polycrystalline LSMO/MgO films.
5. Electrical and magnetoresistive properties of point-like Ag/LSMO contact are caused mainly by the so-called spreading resistance originating from a small volume of the manganite material at the Ag/LSMO interface caring the highest current density. The highest magnetoresistance of point-like contact, $MR_{Ag/LSMO}$, up to 13% ($\mu_0 H$ = 0.73 T) has been measured at T = 295 K by applying 3 point-probe method. It was found that highly resistive surface layers appearing on the LSMO film surface result increase of contact resistance, $R_{Ag/LSMO,}$ and decrease of the $MR_{Ag/LSMO}$ values.
6. Thin films of the organic semiconductors, namely, Alq_3, several organic compounds based on naphthalene diimide (PEPK, FCAND ir POANT) and perimidine (BPBC, EBC) have been prepared on crystalline *n*-Si, *p*-Si and STON substrates by applying thermal evaporation and spin coating technologies. Comparative study of current-voltage relations have been performed for the prepared hybrid diode structures. Schottky-type behaviour with clearly defined rectifying properties has been indicated for the Al/Alq_3/*n*-Si diode structures.
7. Hybrid organic-inorganic Al/Alq_3/*n*-Si, Al/Alq_3/*p*-Si diode structures demonstrate increased barrier height (0.85÷1.0 eV and 0.9÷1.1 eV, respectively) and reduced ideality factor, *n*, values compared to similar Al/*p*-Si and Al/*n*-Si device structures. Increased barrier height values: certify importance of interface dipole (induced by polar Alq_3 molecules) on barrier formation while lower *n* values show reduced influence of localized states on Si surface.
8. Al/Alq_3/*p*-Si diode structures demonstrated significantly higher series resistance values compared to similar Al/Alq_3/*n*-Si device structures. This experimental facts

certifies that Alq_3 is basically an electronic conductor, i.e. electrical resistance of the compound is higher when electronic holes are injected from *p*-Si substrate.

9. Heterojunctions demonstrating clearly defined Schottky type behaviour have been prepared by growing manganite films on conducting STON substrates. The resultant Schottky barrier height Φ_{B0}=0.81 eV has been estimated for the LCMO/STON structures from current-voltage relations, measured at room temperature.
10. It was found that both diode-like electrical properties and electrical stability of the LSMO/*n*-Si and LCMO/*n*-Si heterostructures may be improved by introducing ultrathin ($d \cong 5$ nm) layers of insulating $LaMnO_3$ and ZrO_2<Y> in between the manganite films and the substrate.
11. Nonlinear electrical properties indicated for the Ag/Alq_3/LSMO structures have been explained taking into account space-charge limited current in highly resistive Alq_3 interlayer. Significant negative magnetoresistance (up to 11 % at T = 240 K and $\mu_0 H$ = 1 T) measured for the device structure have been explained taking into account importance of leakage current and reduced carrier density at LSMO film surface caused by the adjacent Alq_3 layer.

References

[1] Dorr, K., Ferromagnetic manganites: spin-polarized conduction versus competing interactions. *J. Phys. D: Appl. Phys.* **39**, R125–R150 (2006).

[2] Haghiri-Gosnet, A.-M., and Renard, J.-P., CMR manganites: physics, thin films and devices. *J. Phys. D: Appl. Phys.* **36**, R127–R150 (2003).

[3] Vardeny, Z.V., *Organic spintronics*. Ed. by Z. V. Vardeny. CRC Press, London, New York, 2010.

[4] Dagotto, E., Hotta, T., and Moreo, A., Colossal magnetoresistant materials: the key role of phase separation. *Phys. Rep.* **344,** 1 (2001).

[5] Zhang, P., On the spreading resistance of thin film contacts. *IEEE Trans. Electron Devices* **59**(7), 1936–1940 (2012).

[6] Rhoderick, E.H., *Metal-Semiconductor contacts*. Oxford University Press, Oxford, 1978.

[7] Simons, J.G., Generalized formula for the electric tunnel effect between similar electrodes separated by a thin insulating film. *J. Appl. Phys.* **34**, 1793 (1963).

[8] Aydına, M.E., Turut A., Microelectronic Engineering 84, 2875 (2007).

About the author

Name, surname	**Irina ČERNIUKĖ**
Date of birth	March 31, 1981.
Citizenship	Lithuania
Address	Užukulpio km. 2, Lentvario sen., Trakų raj.
Phone:	+370 674 466 29
e-mail:	lapkina@gmail.com

Education

2007-2015	PhD student in Center for Physical Sciences and Technology, Semiconductors Physics Institute. (Vilnius University)
Sept. 2005-Feb. 2006	PhD student at Kaunas University of Technology
June 2005	Master of Physics degree in Applied Physics (cum laude), Kaunas University of Technology.
June 2003	Bachelor's degree in Applied Physics, awarded at Kaunas University of Technology.
	Teaching assistant / tutor at Kaunas University of Technology
Teaching	The primary duty was serving as a co-instructor for teaching undergraduate students in laboratories.
2005-2006	Courses taught: 1) Introductory Physics I (Mechanics, Thermodynamics, Electromagnetism); 2) Introductory Physics II (Optics and Atomic Physics).

REZIUMĖ

Šiuo metu daug dėmesio skiriama naujų elektronikos (nanoelektronikos) krypčių: sukinių elektronikos arba spintronikos, molekulinės elektronikos, taip pat organinės spintronikos vystymui. Spintronikos prietaisams reikalingi elektrai laidūs feromagnetikai. Pageidautina, kad jų Kiuri temperatūros T_C vertės būtų aukštesnės už kambario temperatūrą ir kad juose esančių krūvininkų sukiniai feromagnetinėje būsenoje būtų orientuoti. Tokiomis savybėmis pasižymi manganitas $La_{0,67}Sr_{0,33}MnO_3$ (LSMO), kurio T_C vertė 370 K. Panaudojant manganitų plonuosius sluoksnius ir sudarant daugiasluoksnius darinius iš dviejų laidžių feromagnetinių elektrodų, atskirtų nemagnetiniu organiniu sluoksniu, tikimasi sukurti įvairios paskirties magnetinio lauko jutiklius bei magnetinės atminties elementus, kurie dėl ilgesnių sukinių relaksacijos laikų būtų efektyvesni, spartesni, naudotų mažiau energijos. Vis dėlto, bandant pritaikyti manganitus ir organinius puslaidininkius spintronikoje, iškyla problemų dėl technologinio medžiagų nesuderinamumo, pastebėta naujų reiškinių, kuriems išaiškinti reikėtų detaliau ištirti krūvininkų pernašą tarpfazinėse srityse. Tokių problemų sprendimui ir skiriamas šis disertacinis darbas.

Pirmasis skyrius skirtas mokslinės literatūros apžvalgai. Aprašomos manganitų ir organinių puslaidininkių elektrinės ir magnetovaržinės savybės, nurodyti pagrindiniai modeliai, paaiškinantys elektros transporto mechanizmus ir magnetovaržos prigimtį. Apžvelgti moksliniai darbai, kuriuose nagrinėjamos heterosandūrų su manganitais ir organiniais puslaidininkiais magnetovaržinės savybės.

Antrajame skyriuje aprašyti šiame darbe naudoti plonųjų sluoksnių auginimo būdai, apžvelgiami elektrinių kontaktų gamybos ypatumai. Trumpai apibūdinti darbe panaudoti kristalinės struktūros, elektrinių bei magnetinių savybių tyrimo metodai.

Trečiajame skyriuje aprašyti LSMO sluoksniai, užauginti magnetroninio dulkinimo būdu įvairiose temperatūrose ant kristalinių MgO(001) padėklų, esant dideliam (~8,0%) kristalinių gardelių nesutapimui. Detaliai analizuojama sluoksnių struktūra, kristalitų ir tarpkristalitinių sričių įtaka sluoksnių elektrinei varžai ir magnetovaržai 78÷330 K temperatūrų ruože.

Ketvirtame skyriuje aprašytas mažo ploto Ag/$LSMO_3$ sandūrų sudarymas ir jų elektrinės bei magnetovaržinės savybės.

Penktasis skyrius skirtas Alq_3, taip pat naftaleno diimido ir perimidino grupės junginių plonųjų sluoksnių gaminimui ant elektrai laidžių *n*-Si, *p*-Si ir *n*-$SrTiO_3$<Nb> (STON) padėklų naudojant terminio garinimo vakuume ir tirpalo skleidimo technologijas. Aprašyti lyginamieji pagamintų diodinių darinių voltamperinių charakteristikų tyrimai ir nustatyti svarbiausi šių darinių parametrai.

Šeštajame skyriuje aprašyti hibridiniai plonasluoksniai diodiniai *p*-*n* ir *p*-*i*-*n* dariniai, sudaryti ant STON, *n*-Si, *p*-Si padėklų iš elektrai laidžių magnetinių medžiagų - LSMO ir LCMO, dielektrinių oksidų – ZrO_2<Y> ir $LaMnO_3$ bei organinio puslaidininkio - Alq_3.

Tyrimų objektas

- Manganitų: (LSMO, LCMO), organinių puslaidininkių (Alq_3 taip pat kai kurių naftaleno diimido: PEPK, FCAND ir POANT ir perimidino: BPBC, EBC grupės junginių) plonieji sluoksniai ir jų dariniai.
- Diodinių *p*-*n* ir *p*-*i*-*n* darinių iš manganitų, neorganinių (*n*-Si, *p*-Si, STON) ir

organinių puslaidininkių struktūrinės, elektrinės ir magnetovaržinės savybės.

Darbo tikslai ir uždaviniai

- Ištirti kaip keičiasi LSMO sluoksnių kristalinė sandara, elektrinė varža ir jos temperatūrinė priklausomybė taip pat magnetovaržinės savybės auginant LSMO sluoksnius magnetroninio dulkinimo būdu įvairiose temperatūrose (T_s=550÷800°C) ant kristalinių MgO(001) padėklų.
- Išaiškinti tarpkristalitinių ribų įtaką auginamų LSMO/MgO sluoksnių elektrinei varžai ir magnetovaržai esant silpniems ($\mu_0 H$<0,2T) ir stipriems ($\mu_0 H$>0,2T) magnetiniams laukams.
- Ištirti mažo ploto Ag/LSMO sandūrų elektrines ir magnetovaržines savybes.
- Sukurti plonasluoksnių diodinių darinių su manganitais (LSMO, LCMO) ir organiniais puslaidininkiais technologiją, ištirti jų elektrines savybes.

Siekiant šių tikslų, buvo sprendžiami tokie uždaviniai:

- Buvo atliekami lyginamieji orientuotų ir polikristalinių LSMO/MgO(001) sluoksnių elektrinių savybių tyrimai. Siekiant išaiškinti kristalitų ir tarpkristalitinės srities įtaką elektrinėms ir magnetovaržinėms savybėms įvairiose temperatūrose, buvo atlikti kompleksiniai bandinių kristalinės struktūros taip pat jų elektrinių savybių tyrimai.
- Naudojant terminio garinimo vakuume ir tirpalo skleidimo technologijas ant elektrai laidžių *n*-Si, *p*-Si ir STON padėklų buvo gaminami organinių puslaidininkių: Alq_3 taip pat naujai susintetintų naftaleno diimido (PEPK, FCAND ir POANT) ir perimidino (BPBC, EBC) grupės junginių plonieji sluoksniai. Buvo atliekami lyginamieji sudarytų diodinių darinių voltamperinių charakteristikų tyrimai ir nustatomi svarbiausi šių diodinių darinių elektriniai parametrai.
- Buvo gaminami plonasluoksniai diodiniai *p-n* ir *p-i-n* dariniai, sudaryti iš elektrai laidžių magnetinių medžiagų - LSMO, LCMO, nemagnetinių puslaidininkinių medžiagų - STON ir *n*-Si(100), dielektrinių oksidų - ZrO_2<Y> (YSZ) ir $LaMnO_3$ (LMO) ir organinio Alq_3 puslaidininkio bei tiriamos pagamintų diodinių darinių elektrinės ir magnetovaržinės savybės.

Darbo mokslinis naujumas ir praktinė vertė

- Išaiškinta tarpkristalitinių sričių įtaka įvairios kristalinės kokybės LSMO/MgO sluoksnių elektrinėms ir magnetovaržinėms savybėms.
- Pagaminti naujai susintetintų naftaleno diimido ir perimidino grupių organinių junginių plonieji sluoksniai taip pat hibridiniai diodiniai M/OP/*n*-, *p*-Si dariniai. Ištirtos jų elektrinės savybės.
- Sukurtos hibridinių magnetinių oksidų ir organinių puslaidininkių plonųjų sluoksnių ir jų hibridinių diodinių darinių technologijos. Išaiškintos galimybės minėtas medžiagas integruoti į puslaidininkinius mikroelektronikos prietaisus ir panaudoti naujų elektronikos ir spintronikos prietaisų gaminimui.
- Kokybiškam Šotkio diodui būdingos netiesinės LCMO/YSZ/*n*-Si darinių savybės įgalina panaudoti magnetinius manganitų sluoksnius integriniuose Si mikroelektronikos grandynuose.
- Ištirtos magnetovaržinės mažo ploto Ag/LSMO sandūrų savybės atveria naujas

galimybes jas pritaikyti kambario temperatūroje veikiančių mažų matmenų magnetinio lauko jutiklių kūrimui.

Disertacijos gynimui pateikiami šie **ginamieji teiginiai**:

1. Polikristalinių LSMO/MgO sluoksnių elektrines savybes, esant žemoms temperatūroms ($T<<T_C$), lemia elektriškai nevienalytės tarpkristalitinės ribos. Tarpkristalitinių ribų magnetovaržines savybes, esant silpniems ($\mu_0 H<0.2$T) ir stipriems ($\mu_0 H>0.2$T) magnetiniams laukams, paaiškina dviejų erdvėje išskirstytų lygiagrečiai sujungtų kanalų modelis.
2. Mažo ploto Ag/LSMO sandūrų elektrines ir magnetovaržines savybes paaiškina vadinamoji sutelktoji elektrinė varža. Ją lemia po elektrodu esantis ribotas medžiagos tūris, kuriame srovės tankis yra didžiausias.
3. Didesnes hibridinių Al/Alq_3/*n*-Si, Al/Alq_3/*p*-Si darinių potencinio barjero reikšmes (atitinkamai 0,9 eV ÷ 1,1 eV ir 0,77 eV ÷ 0,91 eV) lyginant su diodinių Al/*n*-Si ir Al/*p*-Si darinių vertėmis (atitinkamai 0.68 eV ir 0.77 eV) lemia polinių Alq_3 molekulių indukuoti dipoliniai momentai.
4. Šotkio sandūros, sudarytos epitaksiškai auginant LSMO ir LCMO sluoksnius ant elektrai laidžių monokristalinių STON padėklų, pasižymi mažomis nuotėkio srovės vertėmis. Diodinių (LSMO, LCMO)/*n*-Si darinių nuotėkių sroves galima žymiai sumažinti tarp *n*-Si padėklo ir ant jo auginamų LSMO ir LCMO manganitų sluoksnių įterpiant plonus ($d \leq 5$ nm) dielektrinių $LaMnO_3$ (LMO) ir Y_2O_3(8 mol % ZrO_2) (YSZ) junginių tarpsluoksnius.

Disertacijos struktūra

Bendra darbo apimtis - 134 psl. Darbą sudaro įvadas, literatūros apžvalga, metodikos ir tyrimo rezultatų skyriai, išvados, literatūros ir publikacijų darbo tema sąrašai. Darbe yra pateikti 62 paveikslai, 13 lentelių, 18 formulių ir 118 šaltinių literatūros sąrašas.

Darbo aprobacija ir autorės įnašas

Disertacijos tema paskelbti 4 straipsniai referuojamuose moksliniuose žurnaluose, įtrauktuose į Thomson ISI duomenų bazę, 4 publikacijos išspausdintos tarptautinėse ir respublikinėse konferencijų medžiagose. Tyrimo rezultatai buvo viešinami eilėje nacionalinių ir tarptautinių konferencijų.

Disertacijos autorė prisidėjo gaminant manganitų taip pat organinių junginių plonuosius sluoksnius bei jų darinius. Fizikiniai eksperimentiniai tyrimai buvo atliekami kartu su kitais publikacijų bendraautoriais. Autorė taip pat atliko pradinę duomenų analizę, modelinius tyrimus, dalyvavo rezultatų aptarime ir kartu su bendraautoriais ruošė tyrimų medžiagą spaudai.

IŠVADOS

1. Parodyta, kad aukštadažnio magnetroninio dulkinimo būdu 800°C temperatūroje ant kristalinių MgO(001) padėklų, esant dideliam (~8,0 %) kristalinių gardelių nesutapimui, galima užauginti (001) plokštumoje orientuotus LSMO sluoksnius, kurie savo elektrinėmis savybėmis prilygsta epitaksiniams LSMO sluoksniams,

auginamiems ant suderintų gardelių padėklų, tuo tarpu auginant LSMO sluoksnius žemesnėse temperatūrose (T_s=750÷550°C) ant tokių pačių padėklų užauga polikristaliniai LSMO sluoksniai, kuriuose tarp (001) orientuotų sričių yra įsiterpę kitos (011) orientacijos kristalitai.

2. Ištirta kristalitų ir tarpkristalitinių sričių įtaka sluoksnių elektrinei varžai ir magnetovaržai plačiame temperatūrų ruože. Nustatyta, kad mažesnes polikristalinių sluoksnių vertes kambario temperatūroje lemia papildoma tarpkristalitinių sričių varža, kuri šioje temperatūrų srityje silpnai priklauso nuo magnetinio lauko.
3. Silpno lauko magnetovaržos reiškinys polikristaliniuose LSMO sluoksniuose paaiškintas krūvininkų su orientuotais sukiniais tuneliavimu per magnetiniu lauku valdomą tunelinį barjerą, susidarantį technologinio proceso metu riboje tarp gretimų skirtingai orientuotų kristalitų. Tuo tarpu žymi polikristalinių sluoksnių magnetovarža, esant žemoms temperatūroms ir stipriems magnetiniams laukams, buvo susieta su šuoline krūvininkų pernaša per tarpkristalitines sritis, pasižyminčias sumažinta krūvininkų koncentracija.
4. Tarpkristalitinių ribų magnetovarža, stebėta tuo pačiu metu silpnuose (LFMR) ir stipriuose (HFMR) magnetiniuose laukuose, paaiškinta pasitelkus dviejų lygiagrečiai sujungtų elektrai laidžių kanalų modelį. Aptarta galima fazinio išsisluoksniavimo reiškinio įtaka nevienalytės tarpkristalitinės terpės susidarymui tiriamuosiuose polikristaliniuose LSMO sluoksniuose.
5. Nustatyta, kad mažo ploto Ag/LSMO sandūrų elektrines ir magnetovaržines savybes paaiškina vadinamoji sutelktoji elektrinė varža R_{spr}. Ją lemia po elektrodu esantis ribotas medžiagos tūris, kuriame srovės tankis yra didžiausias. Didžiausios tokių sandūrų magnetovaržos vertės, siekiančios 13 % (kai $\mu_0 H$ = 0,73 T), buvo išmatuotos 295 K temperatūroje naudojant 3-jų elektrodų būdą. Nustatyta, kad sandūros magnetovarža sumažėja susidarius padidintos elektrinės varžos paviršiniam manganito sluoksniui.
6. Naudojant terminio garinimo vakuume ir tirpalo skleidimo technologijas ant elektrai laidžių *n*-Si, *p*-Si ir STON padėklų pagaminti Alq_3, taip pat naujai susintetintų naftaleno diimido (PEPK, FCAND ir POANT) ir perimidino (BPBC, EBC) grupės junginių plonieji sluoksniai. Lyginimo savybės, voltamperinių charakteristikų netiesiškumas yra ryškiausi diodiniams dariniams su Alq_3.
7. Hibridiniams Al/Alq_3/*n*-Si ir Al/Alq_3/*p*-Si dariniams su vakuume užgarintais Alq_3 sluoksniais išmatuotos didesnės potencinio barjero reikšmės (atitinkamai 0,9 eV ÷ 1,1 eV ir 0,77 eV ÷ 0,91 eV) ir mažesnės idealumo faktoriaus *n* vertės lyginant su panašiais Al/*n*-Si ir Al/*p*-Si dariniais. Padidėjusios barjero aukščio vertės rodo, kad sandūroje atsiranda polinių Alq_3 molekulių indukuoti dipoliai, o sumažėjusios *n* vertės rodo, kad įterpus OP sluoksnį sumažėja silicio paviršinių būsenų įtaka.
8. Nustatyta, kad diodinių Al/Alq_3/*p*-Si darinių nuosekliosios diodo varžos R_s vertės yra daugiau kaip eile didesnės lyginant su Al/Alq_3/*n*-Si darinių vertėmis. Šis dėsningumas paaiškintas tuo, kad Alq_3 yra elektroninis laidininkas ir todėl jo elektrinė varža yra didesnė prijungus įtampą tiesiogine kryptimi, t. y. kai iš *p*-Si į OP yra injektuojamos skylės.
9. Kokybiškos Šotkio sandūros buvo pagamintos magnetroninio dulkinimo būdu auginant plonuosius LCMO sluoksnius ant elektrai laidžių monokristalinių STON padėklų. Iš kambario temperatūroje atliktų voltamperinių charakteristikų matavimų įvertintas susidariusios LCMO/STON sandūros barjero aukštis Φ_{B0}=0,81 eV.

10. Diodiniai dariniai, kurie buvo gauti auginant LSMO ir LCMO sluoksnius ant *n*-Si padėklų, pasižymėjo palyginti mažomis elektrinės varžos vertėmis. Tai rodo, kad dalis srovės tokiuose dariniuose teka ne pro potencinį barjerą, o per mažos elektrinės varžos sritis. Mūsų tyrimai parodė, kad galima žymiai sumažinti tokių diodinių darinių nuotėkio sroves, pagerinti jų stabilumą, o taip pat padidinti srovės lyginimo savybes įterpiant plonus ($d \leq 5$ nm) dielektrinių LMO ir YSZ junginių tarpsluoksnius.
11. Netiesinės Ag/Alq_3/LSMO sandūrų voltamperinės charakteristikos paaiškintos atsižvelgiant į erdvinio krūvio ribotas sroves didelės elektrinės varžos organiniame Alq_3 sluoksnyje. Palyginti didelės Ag/Alq_3/LSMO sandūros neigiamos magnetovaržos vertės (siekiančios 11 %, kai $T = 240$ K ir $\mu_0 H = 1$ T) susietos su lokalinėmis nuotėkių srovėmis ir nuskurdinto paviršinio LSMO sluoksnio savybėmis.